J Solid State Electrochem (2008) 12:1637–1644
DOI 10.1007/s10008-008-0534-2

ORIGINAL PAPER

EIS characterization of corrosion processes of titanium and alloy UNS N10276 in sour environments

J. Mendoza-Canales · J. Marín-Cruz

Received: 27 November 2007 / Accepted: 19 February 2008 / Published online: 28 March 2008

Abstract Titanium grade 2 (UNS R50400) and nickel-based alloy (UNS N10276) were electrochemically investigated to explore their corrosion susceptibility in sour (H_2S) environments typically found on atmospheric distillation units in crude oil refineries. Electrochemical impedance spectroscopy (EIS) was used to attain the experimental results. Two individual solutions (0.05 mol/l HCl and 0.05 mol/l HCl+500 ppm H_2S) were utilized in the laboratory work to replicate major corrosive agents present in actual atmospheric distillation systems for a characteristic heavy crude oil produced in Mexico. Metals were examined at pH 1.5, 4, 6, 8, and 10 values for the two solutions to identify the effects of pH modification on corrosion processes. The results disclosed that each metal has dissimilar corrosion susceptibility depending on the pH of the environment. Therefore, pH intervals for which every metal holds minimum susceptibility were identified. In addition, the convenience of controlling the pH of streams within a definite interval (5.5–6.5) is discussed and a few hints on decision-making to improve the operation of atmospheric distillation units are also explained.

J. Mendoza-Canales
Instituto Mexicano del Petróleo,
Dirección de Investigación y Posgrado,
Eje Central Lázaro Cárdenas Norte, 152,
C.P. 07730, México D.F., México
e-mail: jmendoza@imp.mx

J. Marín-Cruz (✉)
Instituto Mexicano del Petróleo,
Coordinación de Ingeniería Molecular,
Competencia de Química Aplicada,
Eje Central Lázaro Cárdenas Norte 152,
C. P. 07730, México D.F., México
e-mail: jmarin@imp.mx

Keywords Sour environment · Titanium · Nickel-based alloy · Overhead system corrosion · EIS

Introduction

Atmospheric distillation columns and overhead condensation systems play a fundamental role in refineries because they are the primary process equipment which directly undergoes the detrimental consequences of contaminants that crude oils contain even after the desalting and dehydration processes. A simple flow diagram of the system is shown in Fig. 1.

In this system, corrosion occurs due to the combined action of hydrochloric acid (HCl) formed by the hydrolysis of $MgCl_2$ and $CaCl_2$, and hydrogen sulfide (H_2S) contained in sour crude oils. These are strong acids able to cause significant corrosion deterioration of steels and other metals. Substances such as napthenic acids, CO_2, and others are present in crude oils; nevertheless, HCl and H_2S are considered as the major corrosive species in the system [2–14].

In recent years, this corrosion problem has become more serious due to the fact that there is a growing worldwide need to refine heavier crudes. In general terms, heavier crudes have superior API gravities and enlarged amounts of metals, asphaltenes, and sulfur, which are more difficult to be diminished during the refining processes.

Several corrosion experiences have been reported for the refining of crude oils produced in varied sites of the world and processed under certain conditions [15–20]. However, no reports were found for defined conditions of Mexican refineries which, nowadays, are compelled to process heavy and extra heavy crude oils (API<12; dissolved salts 2.5–80 ptb; total sulfur 3.7–5.3 wt%) whose properties are

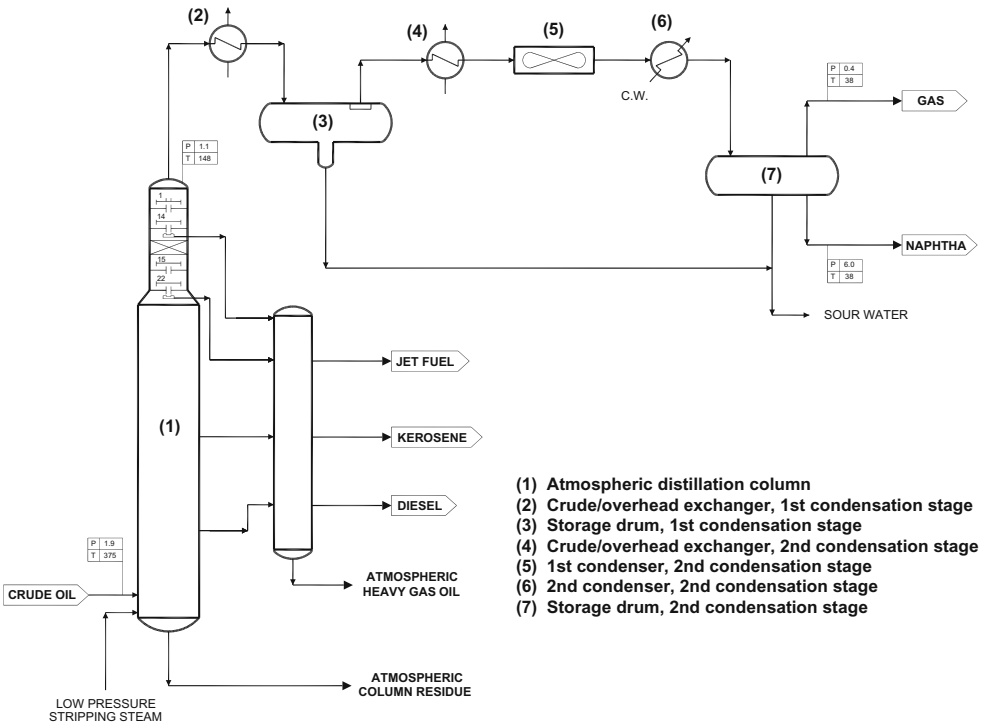

Fig. 1 Typical flow diagram of atmospheric distillation column and two-stage condensation system

notably contrasting with those of lighter crude oils produced in other regions of the world (API ranging from 16 up to 52; dissolved salts 0.2–45 ptb; total sulfur 0.4–3.0 wt%). In addition, such heavier crude oils have increased quantities of metals (V and Ni) and asphaltenes [21–28].

In this work, two commercially manufactured metals—titanium UNS[1] R50400 and alloy UNS N10276—were electrochemically explored to determine their corrosion susceptibility in sour environments typical of crude oils and refining features specific to Mexican circumstances.

Electrochemical impedance spectroscopy (EIS) was utilized to characterize the corrosion processes for each metal–environment array quite closely as they evolve in nature. It was also used to determine the effects of the pH of the environment on corrosion phenomena and to identify the consequences of hydrogen sulfide on them.

The aim of this work is to offer a methodology—based on the corrosion susceptibility of metals—to select materials of construction for atmospheric distillation units in the refining industry.

Materials and methods

To define the concentrations of hydrochloric acid (HCl) and hydrogen sulfide (H_2S) to be utilized in preparing laboratory solutions, a statistical analysis was made before this work to determine the amounts of dissolved salts and water content for a crude feed to the atmospheric distillation column in a refinery that processes a heavy crude oil typically produced in Mexico. From this determination, other higher and lower values were tested to identify definite concentrations of HCl and H_2S which caused both solutions to be the most corrosive [29–30]. The resulting molar concentrations were 0.05 mol/l HCl and 0.05 mol/l HCl+500 ppm H_2S (sour environment).

Both solutions yielded innate pH values of approximately 1.5 in the blank solutions and were subsequently adjusted to 4, 6, 8, and 10 by adding a neutralizing amine (monoethanolamine [MEA]). MEA is frequently used during normal plant operation in refineries to control the pH of the process streams.

In all electrochemical experiments, a conventional three-electrode cell was employed with a saturated calomel reference electrode (SCE). The counter electrode was a graphite bar. The reference and counter electrodes were arranged in separate compartments. The working electrodes were titanium grade 2 and alloy UNS N10276 discs each embedded in a Teflon tube to allow for free rotation. Titanium grade 2 is designated as UNS R50400 and is a metal having a nominal commercial purity of 99%. The

[0] The unified numbering system (UNS) was conceived and established by ASTM and SAE. It is an alphanumeric code system whose designation starts with a letter followed by five digits and applies to any alloy. A distinctive UNS number is assigned to each alloy to specify its chemical composition [1].

chemical composition (nominal) of nickel-based alloy UNS N10276 is shown in Table 1.

The exposed area of the working electrode was 0.5 cm^2. The electrode surface was cleaned by grinding using 600-grit water-cooled silicon carbide papers followed by a 5-min soak in ultrapure deionized water. This cleaning process was repeated for the working electrode before each experiment to ensure clean and uniform surface. Chemical reagents were analytical grade dissolved in Millipore-Q ultrapure deionized water (Millipore-Q system; resistivity=18 MΩ). The experiments were performed using an Autolab model PGSTAT30 potentiostat/galvanostat. System response and data processing were achieved by means of the frequency response analyzer (FRA) software.

It has been broadly reported that corrosion phenomena are influenced by hydrodynamic flow conditions. The mass transfer rate of the reactant from the bulk to the metal surface depends on the hydrodynamic conditions and, hence, on the diffusion layer thickness. An increase in flow rate decreases the diffusion layer thickness and accelerates electrochemical reactions of species (particularly oxidants) on a metal surface [31–35]. Therefore, in this investigation, the working electrodes were rotated at 2,000 rpm constant speed during every experiment to attain two purposes: to control the diffusion layer thickness in the electrochemical interface and to reproduce flow conditions commonly found in equipment and pipelines of real-life plants. Similarly, because temperature has a crucial influence on corrosion processes in metals, all experiments were carried out maintaining the temperature at 40 °C.

EIS characterization was carried out under the following conditions: amplitude of ±10 mV, frequency range from 10 kHz to 10 mHz, and 5 h immersion time of the working electrode in the solution.

Results and discussion

The description of the analysis of the EIS spectra obtained for titanium UNS R50400 and alloy UNS N10276 at pH 1.5, 4, 6, 8 and 10 values of two individual environments (0.05 mol/l HCl and 0.05 mol/l HCl+ 500 ppm H_2S) is presented in the following paragraphs. For simplicity reasons, the figures only include pH 1.5, 6, and 10 values.

Regarding sour environment (i.e., 0.05 mol/l HCl+ 500 ppm H_2S), Figs. 2a and 3a for titanium UNS R50400 and alloy UNS N10276, respectively, reveal that active corrosion behaviors arise at pH 1.5. The smallest activity is found at pH 6 and is evidenced by the maximum values of real and imaginary impedances. At pH 10, an apparent reactivation of the surface of the metals occurs. Real and imaginary impedance values for titanium are greater than those for alloy UNS N10276, thus proving that the former is less susceptible to corrosion for the explored pH interval.

In Bode module plots, Figs. 2b and 3b, two time constants—the first emerging at intermediate frequencies and the second at low frequencies—are visible at pH 1.5 and 10 for the two metals. However, low-frequency time constant is not perceptible at pH 6, which suggests that it may be virtually overlapped with the intermediate-frequency constant [36–37].

About phase angles, Figs. 2c and 3c show that for both metals two maximum relative angle values occur at pH 6 while not being discernible for the rest of the pH values. The highest delay of current with respect to potential (i.e., maximum value of angle) takes place at pH 1.5 and 10 for titanium; for alloy UNS N10276, it is similar for all three pH values. The greatest width of the capacitive behavior at the intermediate-frequency zone arises at pH 6, which most likely implies that metals experience a decrease of their susceptibility to corrosion at close-to-neutral pH values. This behavior is possibly caused by the alteration of the metal surface due to the formation of corrosion products which—having a nature different to that of the bare metal—retard the relaxation time linked to the electric properties of the surface, thus creating an overlapping of that time with the charge transfer process.

A comparison of spectra shown before with their corresponding ones obtained for the 0.05-mol/l HCl environment (see Figs. 4 and 5) was done. Nyquist plots for alloy UNS N10276, Figs. 3a and 5a, reveal that H_2S causes the surface of the alloy to be more susceptible to corrosion at pH 1.5. On the other hand, H_2S originates lower corrosion susceptibility at pH 6 and 10 that can be a possible consequence of the formation of passive corrosion products on the alloy surface. Bode module plots, Figs. 3b and 5b, demonstrate that alloy suffers alteration in magnitudes particularly at pH 1.5 where H_2S

Table 1 Nominal chemical composition (% weight) of alloy UNS N10276

C	Mn	P	S	Si	Cr	Mo	Co	W	V	Fe	Ni
0.02[a]	1.0[a]	0.04[a]	0.03[a]	0.08[a]	14.5–16.5	15.0–17.0	2.5[a]	3.0–4.5	0.35	4.0–7.0	Balance

[a] Maximum content

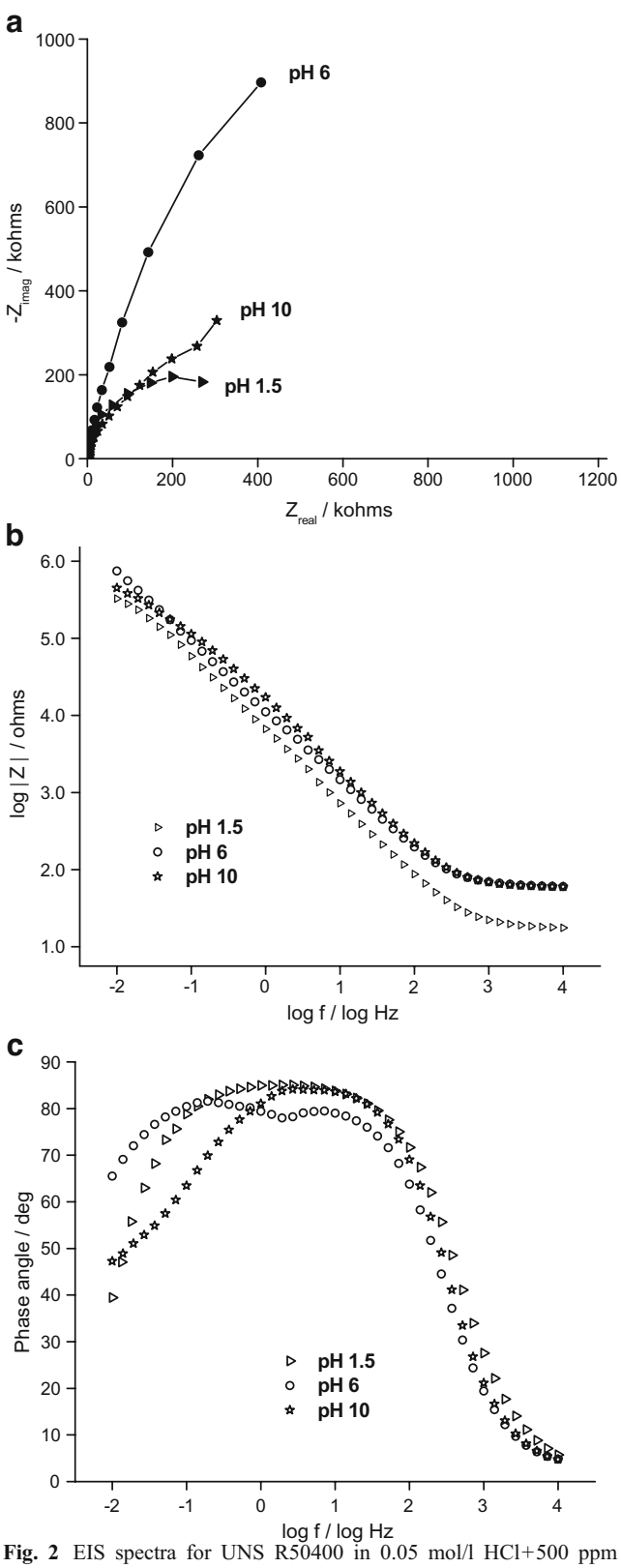

Fig. 2 EIS spectra for UNS R50400 in 0.05 mol/l HCl+500 ppm H_2S; pH 1.5, 6, and 10; 5 h. **a** Nyquist, **b** Bode module, and **c** Bode phase angle plots

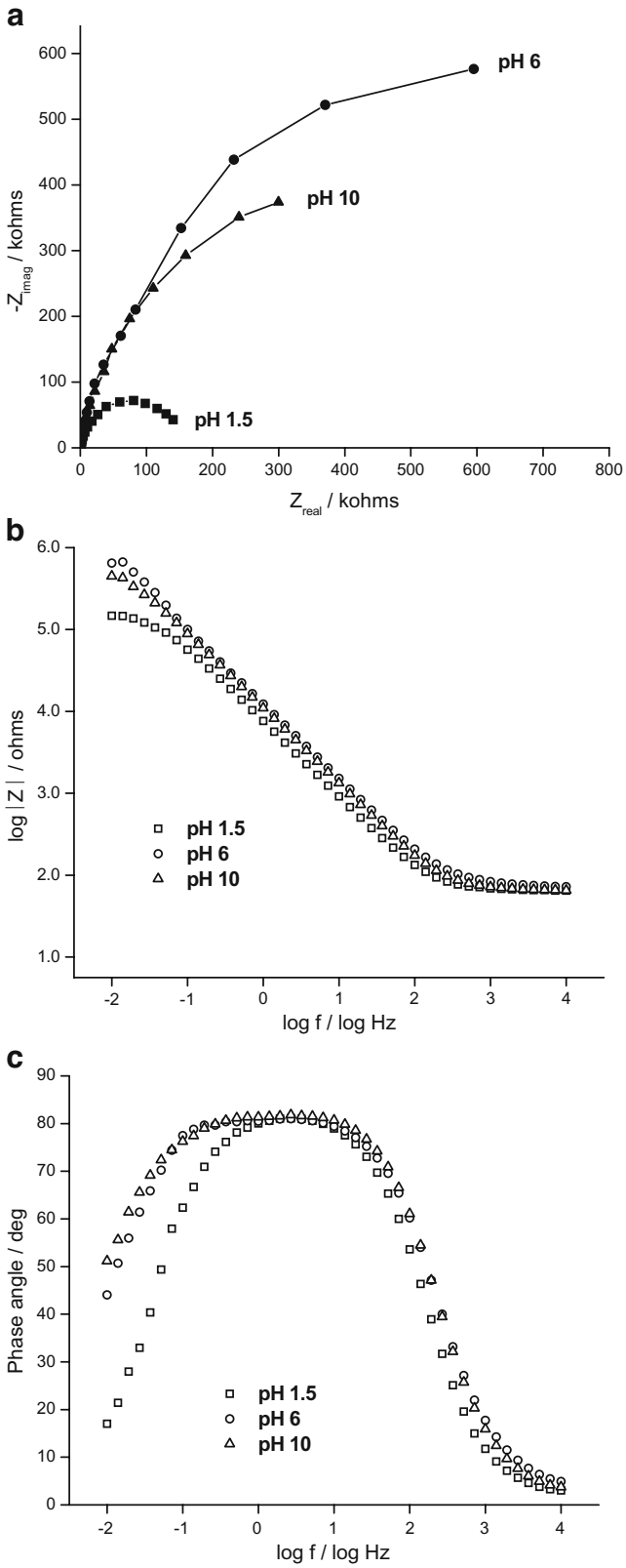

Fig. 3 EIS spectra for UNS N10276 in 0.05 mol/l HCl + 500 ppm H_2S; pH 1.5, 6, and 10; 5 h. **a** Nyquist, **b** Bode module, and **c** Bode phase angle plots

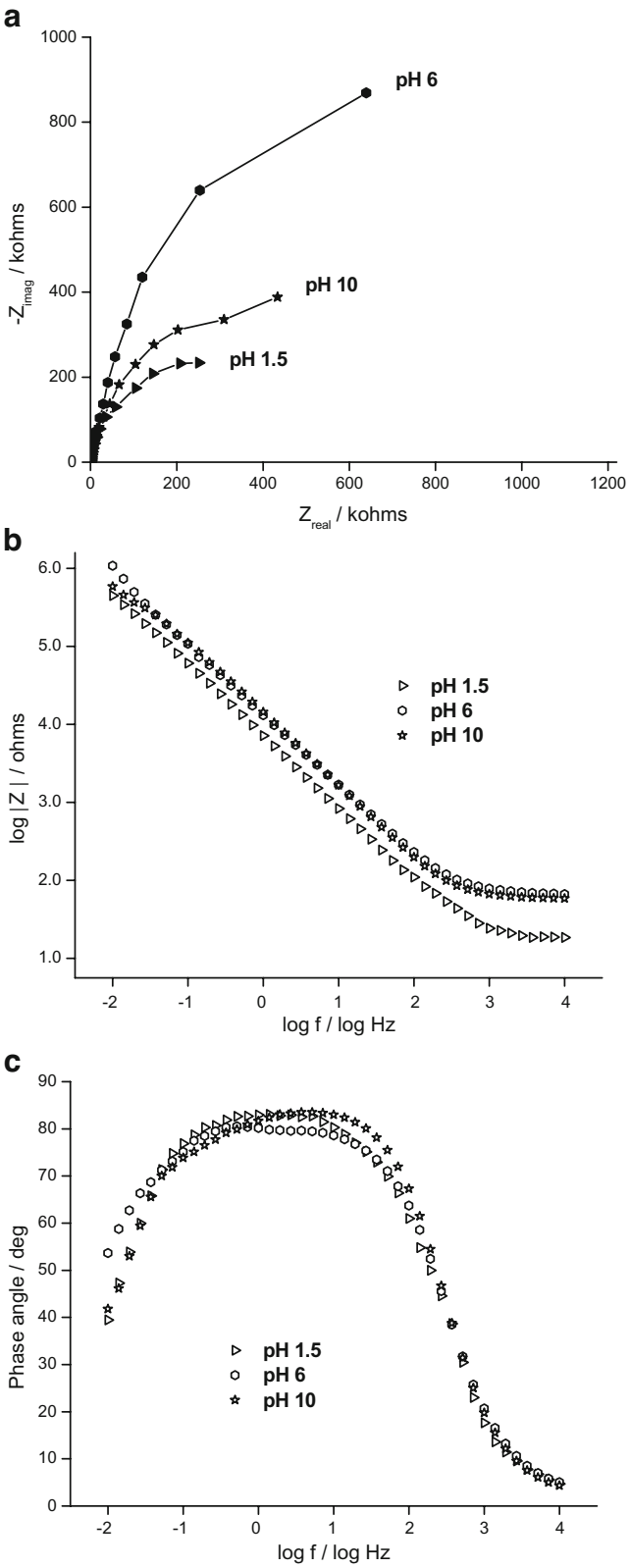

Fig. 4 EIS spectra for UNS R50400 in 0.05 mol/l HCl; pH 1.5, 6, and 10; 5 h. **a** Nyquist, **b** Bode module, and **c** Bode phase angle plots

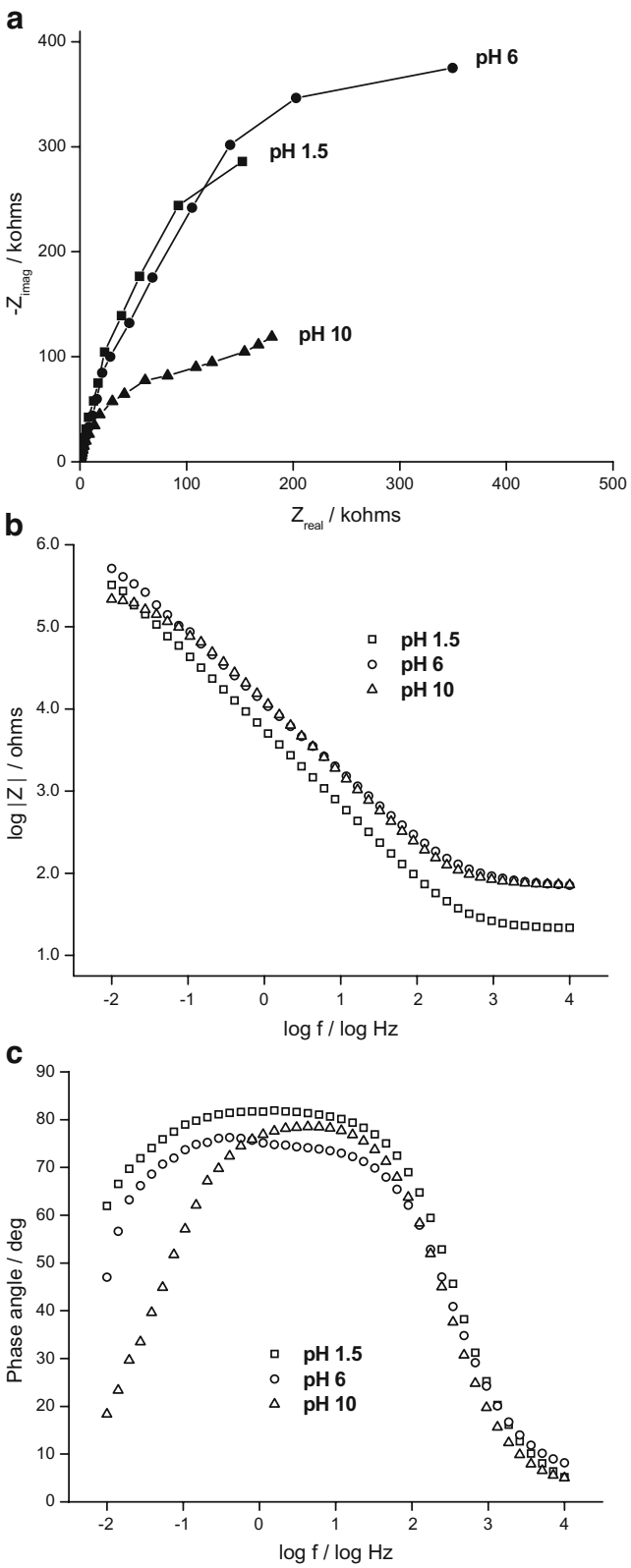

Fig. 5 EIS spectra for UNS N10276 in 0.05 mol/l HCl; pH 1.5, 6, and 10; 5 h. **a** Nyquist, **b** Bode module, and **c** Bode phase angle plots

provokes that the low-frequency time constant, which may be linked to the charging of the electric double layer, becomes visible. Bode phase angle plots, Figs. 3c and 5c, exhibit a significant decrease in the width of capacitive behavior that appears at the intermediate-frequency region; this possibly means that the alloy becomes more susceptible to corrosion at pH 1.5. Nevertheless, the width of that capacitive behavior increases at pH 10, manifesting a contrary effect produced by the H_2S.

With regard to titanium, analysis of spectra (Figs. 2 and 4) exposed that H_2S had *subtle* consequences on the susceptibility to corrosion of the metal when tested at the pH values of the HCl+H_2S environment intended for this work.

Quantitative analysis of electrochemical impedance spectra

The analysis described before gives an idea of the corrosion characterization of metals in terms of qualitative considerations based on the inspection of plots. However, a quantitative explanation of the experimental results helps to deepen the comprehension of corrosion phenomena going on at the interface. Thus, a quantitative interpretation of the EIS spectra is described hereafter.

Fitting of experimental data—i.e., EIS spectra—was performed using customary nonlinear software [38]. A number of "equivalent circuits" were tried to fit data; the best fit was attained for the equivalent circuit as illustrated in Fig. 6. In this circuit, R_s designates the solution resistance, R_x is the resistance of corrosion products, Y_x^0 is the constant phase element (CPE) related to the pseudocapacitance of corrosion products, and R_y and Y_y^0 are the charge transfer resistance and the CPE associated to the pseudocapacitance of the electric double layer, respectively.

The circuit was chosen primarily because the experimental data to be analyzed uncovered the existence of at least *two time constants*. Moreover, it proved to be helpful in simulating the initiation/growth phenomena of corrosion products on metal surfaces and those involving the coexistence of both clean metallic surfaces in direct contact with electrolyte and corrosion products.

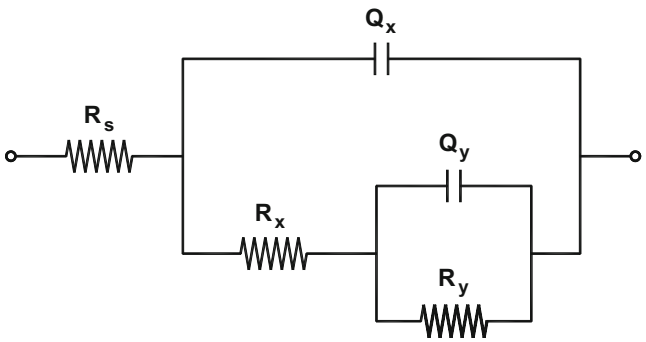

Fig. 6 Equivalent circuit used to adjust the experimental data

Electric parameters obtained from the best fit of the experimental data for titanium UNS R50400 and alloy UNS N10276 in sour solutions are shown in Tables 2 and 3. n_x and n_y stand for the frequency power factors as linked to the pseudocapacitances of corrosion products and of the electric double layer, correspondingly.

Some differences in solution resistance values can be identified for both metals. For titanium (Table 2), resistances are similar except at pH 1.5. For alloy UNS N10276 (Table 3), values are comparable at pH 1.5, 6 and 10; at pH 4 and 8, they are nearly the same and greater than the rest. An explanation for these differences is that each metal–solution interface assumes exceptional properties caused by their reciprocal interaction and are a function of the metallurgical nature of the metal and of the ionic concentration of the solution. The latter is modified by the addition of the neutralizing amine to adjust the pH of the solution.

Relative to the pseudocapacitances Y_x^0 of the corrosion products, the maximum values for the two metals (Tables 2 and 3) take place at pH 6, which may be generated by changes in dielectric permittivities of the corrosion products and/or by larger areas of the metal surface covered by the corrosion products. Frequency power factors exhibit values denoting that the products are able to store charge with efficiencies near to those of the ideal capacitor.

For all pH values, both metals disclose values for charge transfer resistance R_y four orders in magnitude greater than their related resistances of corrosion products R_x. The latter fluctuate in values up to 134.6 Ω/cm^2 except for titanium (Table 2) at pH 10 where a considerably higher resistance (0.178 MΩ/cm^2) is encountered. The reason for this may be that corrosion products experience an increase in their nonconductive (passive) properties. It is important to emphasize that the maximum values of charge transfer resistance are found at pH 6, implying that these two metals possess the *lowest susceptibility* to corrosion particularly at this pH of the HCl+H_2S environment.

Pseudocapacitances of the electric double layer Y_x^0 rise and fall as pH is modified, i.e., they are sensitive to pH

Table 2 Electrical parameters of equivalent circuit attained by fitting experimental data for titanium UNS R50400 in 0.05 mol/l HCl + 500 ppm H_2S at pH values shown

pH	R_s (Ω/cm^2)	Y_x^0 (μF/cm^2)	n_x	R_x (Ω/cm^2)	R_y (MΩ/cm^2)	Y_y^0 (μF/cm^2)	n_y
1.5	17.4	16.8	0.96	29.8	0.41	9.2	0.94
4	59.6	5.4	1.0	80.9	0.92	12.2	0.82
6	58.8	14.2	0.88	58.8	2.89	2.1	1.0
8	57.4	11.9	0.9	58.2	1.08	2.7	1.0
10	61.4	10.2	0.95	178,780	1.79	10.4	0.62

Immersion time: 5 h

Table 3 Electrical parameters of equivalent circuit attained by fitting experimental data for alloy UNS N10276 in 0.05 mol/l HCl + 500 ppm H_2S at pH values shown

pH	R_s (Ω/cm^2)	Y_x^0 (μF/cm^2)	n_x	R_x (Ω/cm^2)	R_y (MΩ/cm^2)	Y_y^0 (μF/cm^2)	n_y
1.5	68.2	9.4	1.0	75.3	0.14	15.2	0.86
4	91.8	7.7	0.92	74.9	0.66	9.2	0.9
6	70.6	11.8	0.89	69	1.11	3.6	0.97
8	95.0	5.6	1.0	134.6	0.94	10.4	0.83
10	65.1	5.1	1.0	33.6	0.99	12.0	0.86

Immersion time: 5 h

Table 5 Electrical parameters of equivalent circuit attained by fitting experimental data for alloy UNS N10276 in 0.05 mol/l HCl at pH values shown

pH	R_s (Ω/cm^2)	Y_x^0 (μF/cm^2)	n_x	R_x (Ω/cm^2)	R_y (MΩ/cm^2)	Y_y^0 (μF/cm^2)	n_y
1.5	21	29.6	0.9	42.6	0.94	4.1	0.98
4	66.8	7.0	0.9	20.1	0.7	13.0	0.88
6	68.4	12.4	0.84	82.2	1.62	4.9	0.88
8	75.4	8.6	0.91	70.8	1.69	7.8	0.85
10	70.9	3.4	1.0	27.5	0.21	12.1	0.85

Immersion time: 5 h

alteration of the environment. Nonetheless, it is interesting to highlight that minimum values for the two metals occur just at pH 6. A feasible cause of this is that the double layer grows in thickness and develops into a stronger layer, thus thwarting to a deeper extent the charge transfer through the interface. This proves that susceptibilities to corrosion for the two metals are *minimal at pH 6* of the HCl+500 ppm of H_2S environment. About the frequency power factors for these metals, values unveil that double layer stores charge with efficiency equivalent to that of an ideal capacitor; an exception involves titanium at pH 10 whose obtained value (0.62) evidences that other conditions—such as roughness or porosity—come into sight and influence double layer response [39].

Based on a comparison of the results provided in Tables 2 and 3 with their analogous ones attained for 0.05 mol/l HCl environment (see Tables 4 and 5), it was found that H_2S originates a *generalized increase* in the corrosion susceptibilities of both metals. This is confirmed by inspecting the charge transfer resistances where values are at the topmost position for all pH values of the 0.05-mol/l HCl environment. Furthermore, for alloy UNS N10276 (Table 5) the highest charge transfer resistance comes up at pH 8 of the 0.05-mol/l HCl environment while in the HCl+H_2S solution (Table 3) that resistance value rises at pH 6. This suggests that H_2S makes the alloy less susceptible to corrosion at close-to-neutral pH values and not at alkaline pH values. In addition, H_2S produces a significant increase in susceptibility of this alloy especially at pH 1.5 because the charge transfer resistance decreases from 0.94 to 0.14 MΩ/cm^2. An opposite effect takes place at pH 10 where charge transfer resistance grows from 0.21 to 0.99 MΩ/cm^2.

Table 4 Electrical parameters of equivalent circuit attained by fitting experimental data for titanium UNS R50400 in 0.05 mol/l HCl at pH values shown

pH	R_s (Ω/cm^2)	Y_x^0 (μF/cm^2)	n_x	R_x (Ω/cm^2)	R_y (MΩ/cm^2)	Y_y^0 (μF/cm^2)	n_y
1.5	18.7	10.4	1.0	18.8	0.55	15.1	0.86
4	66.2	9.9	0.93	88.2	1.89	6.2	0.9
6	64.2	8.6	0.89	29.7	3.64	6.0	0.9
8	56.6	9.1	0.93	86.5	1.28	4.2	0.91
10	59.6	6.4	1.0	79.8	0.93	6.9	0.83

Immersion time: 5 h

Conclusions

EIS was used successfully to characterize the corrosion susceptibility of titanium and alloy UNS N10276 in sour environments. Results unveiled that each metal has *dissimilar susceptibility* to corrosion under equivalent conditions when immersed in characteristic environments found in atmospheric distillation units.

In general terms, repercussions of H_2S on the susceptibility to corrosion are less critical for titanium UNS R50400 than for alloy UNS N10276 at all pH values of both environments—HCl and HCl+H_2S.

Controlling the pH of process streams to maintain them between 5.5 and 6.5 is an *appropriate field practice* because right at pH 6 both metals displayed the lowest susceptibility to corrosion in the HCl+H_2S environment.

At pH 1.5 of the sour environment, the two metals are expected to be remarkably susceptible to corrosion. As said before, this is especially true for alloy UNS N10276 in which the charge transfer resistance value was found to be the lowest. If pH arrived at less acid values (e.g., pH 4), metals would offer moderate susceptibility and corrosion damage will be less serious. If pH attained alkaline values (e.g., pH 8 to 10), both metals will disclose an upsurge in their susceptibility to corrosion that can also be regarded as moderate. Although this susceptibility is foretold to be slightly lower than the one detected at intermediate acid, the pH values of metals will still behave poorly with respect to the response observed at close-to-neutral pH values.

Acknowledgements J. Mendoza-Canales wishes to thank the Dirección de Investigación y Posgrado of the Instituto Mexicano del Petróleo for scholarship granted in working for this research project.

References

1. Gale WF, Totemeier TC (2004) Smithells metals reference book, 8th edn. Butterworth-Heinemann, UK
2. Borgard BG, Bieber SA, Harrell JB (1993) NACE Corrosion/93 Houston, Texas, Paper No. 633
3. Cox WM, Mok WY, Miller RG (1990) NACE Corrosion/90 Houston, Texas, Paper No. 200
4. Edmonson JG, Lehrer SE (1994) NACE Corrosion/94 Houston, Texas, Paper No. 514
5. Fearnside P, Lessard RB, Stonecipher DL (1994) NACE Corrosion/94 Houston, Texas, Paper No. 516
6. French EC, Fahey WF (1983) Mater Perform 22:9
7. French EC, Fahey WF (1979) Oil Gas J 77:67
8. Hausler RH, Coble ND (1972) Hydrocarbon Process 51:108
9. Lindley WA, Strong RC (1986) Oil Gas J 84:112
10. Merrick RD, Auerbach T (1983) Mater Perform 22:15
11. Rue JR, Naeger DP (1990) NACE Corrosion/90 Houston, Texas, Paper No. 211
12. Rue JR, Naeger DP (1987) NACE Corrosion/87 Houston, Texas, Paper No. 199
13. Valenzuela DP, Dewan AK (1999) Fluid Phase Equilib 158:829
14. Schutt HU, Horvath RJ (1987) NACE Corrosion/87 Houston, Texas, Paper No. 198
15. Moiseeva L, Aisin A (2007) Prot Met 43:84
16. Efremov A, Kim S (2006) Prot Met 42:194
17. Zav'yalov VV (2003) Prot Met 39:274
18. Schutt HU, Rhodes PR (1996) Corrosion 52:987
19. Silva CC et al (2007) J Pet Sci Eng 59:219
20. Makarenko VD et al (2007) Chem Pet Eng 43:120
21. Rana MS, Ancheyta J, Maity SK, Rayo P (2007) Pet Sci Technol 25:187
22. Rana MS, Ancheyta J, Maity SK, Rayo P (2007) Pet Sci Technol 25:201
23. Rayo P, Ramírez J, Ancheyta J, Rana MS (2007) Pet Sci Technol 25:215
24. Sánchez Berna AC, Camacho Moran V, Romero Guzmán ET, Yacamán MJ (2006) Pet Sci Technol 24:1055
25. Marín-Cruz J, Cabrera-Sierra R, Pech-Canul MA (2007) J Solid State Electrochem 11:1245
26. Luiz de Assis S, Wolynec S, Costa I (2006) Electrochim Acta 51:1815
27. Chauhan LR, Gunasekaran G (2007) Corros Sci 49:1143
28. Shanbhag AV et al (2007) J Appl Electrochem. DOI 10.1007/s10800-007-9436-8
29. Quej-Aké L, Cabrera-Sierra R, Marín-Cruz J (2006) Proceedings of the 21st Joint International Meeting of the Electrochemical Society, Cancún Quintana Roo, México, 29 October–3 November
30. Quej-Aké L, Cabrera-Sierra R, Arce-Estrada E, Marín-Cruz J (2008) International Journal of Electrochemical Science 3:56
31. Kim YJ, Andresen PL (2003) Corrosion 59:584
32. MacDonald DD (1992) Corrosion 48:194
33. Lin CC, Kim YJ, Niedrach LW, Ramp KS (1996) Corrosion 52:618
34. Lin CC, Smith FR, Ichikawa N, Itow M (1992) Corrosion 48:16
35. Kaesche H (2003) Corrosion of metals: physicochemical principles and current problems. Springer, Berlin
36. Bonnel A, Dabosi F, Deslouis C, Duprat M, Keddam M, Tribollet B (1985) J Electrochem Soc 132:256
37. Pech-Canul MA, Bartolo-Pérez P (2004) Surf Coat Technol 184:133
38. Boukamp BA (1993) User's manual—equivalent circuit version 4.51. Faculty of Chemical Technology, University of Twente, The Netherlands
39. Drogowska M, Ménard H, Lasia A (1996) J Appl Electrochem 26:1169